AGU ADVANCING EARTH AND SPACE SCIENCES

Water Resources Research

RESEARCH ARTICLE
10.1029/2023WR035162

Beyond the Case Study: Characterizing Natural Floodplain Heterogeneity in the United States

Emily P. Iskin[1] and **Ellen Wohl**[1]

[1]Department of Geosciences, Colorado State University, Fort Collins, CO, USA

Key Points:

- Natural floodplains have moderate aggregation of classes, high evenness and intermixing of classes, and a wide range of patch densities
- Floodplain heterogeneity reflects space available on the valley floor and lateral channel mobility

Supporting Information:

Supporting Information may be found in the online version of this article.

Correspondence to:

E. P. Iskin,
Emily.iskin@colostate.edu

Citation:

Iskin, E. P., & Wohl, E. (2023). Beyond the case study: Characterizing natural floodplain heterogeneity in the United States. *Water Resources Research*, *59*, e2023WR035162. https://doi.org/10.1029/2023WR035162

Received 20 APR 2023
Accepted 29 JUL 2023

Author Contributions:

Conceptualization: Emily P. Iskin, Ellen Wohl
Data curation: Emily P. Iskin, Ellen Wohl
Formal analysis: Emily P. Iskin
Funding acquisition: Emily P. Iskin, Ellen Wohl
Investigation: Emily P. Iskin, Ellen Wohl
Methodology: Emily P. Iskin, Ellen Wohl
Project Administration: Emily P. Iskin, Ellen Wohl
Resources: Ellen Wohl
Software: Emily P. Iskin
Supervision: Ellen Wohl
Validation: Emily P. Iskin, Ellen Wohl
Visualization: Emily P. Iskin
Writing – original draft: Emily P. Iskin
Writing – review & editing: Ellen Wohl

Abstract We use the five landscape ecology metrics of aggregation index, percentage of like adjacencies, interspersion and juxtaposition index, patch density, and Shannon's evenness index to assess spatial heterogeneity at 15 floodplains in the continental United States. Assessments are based on floodplain classes and patches delineated remotely using topography and vegetation. Floodplain reaches examined here represent diverse drainage areas, flow regimes, valley geometries, channel planforms, and biomes. We selected sites with minimal direct human alteration. Our objectives are to quantify floodplain spatial heterogeneity; evaluate whether statistically significant patterns are present; and interpret the statistical analyses with respect to the influence of lateral channel mobility and valley-floor space available. We develop a conceptual model of the influences on lateral mobility and space available, and then test specific hypotheses derived from this conceptual model. These natural floodplains have a median aggregation index of 58.8%, median percentage of like adjacencies of 58.5%, median interspersion and juxtaposition index of 74.9%, median density of 1,241 patches/ha, and median Shannon's evenness index of 0.934 (n = 15). In other words, natural floodplains have moderate aggregation of classes, high evenness and intermixing of classes, and a wide range of patch densities. Drainage area, the ratio of floodplain/channel width, elevation, precipitation, total sinuosity, large wood volume, planform, and flow regime emerge as important variables to floodplain heterogeneity. These results highlight the influence of biotic-abiotic interactions in shaping floodplain heterogeneity across diverse river corridors.

Plain Language Summary As river channels move across their valley floors, they create diverse topography including natural levees, cutoff meanders, secondary channels, and floodplain wetlands. These features increase the spatial variability of the floodplain. Many studies indicate that this variability strongly influences habitat abundance and diversity, storage of flood waters and excess nitrate or phosphate, and other floodplain functions. However, no one has systematically measured floodplain variability across multiple rivers and different geographic regions. We measured the variability of natural floodplains at 15 sites in the continental United States using metrics developed by landscape ecologists. We find that natural floodplains have distinctive variability signatures that relate to drainage area, the size of the floodplain, and other characteristics.

1. Introduction

We define floodplain heterogeneity as the spatial variation of geomorphic and vegetation classes and patches across a floodplain (Iskin, 2023; Iskin & Wohl, 2023b). Classes represent distinct types of floodplain habitats that blend geomorphic features and vegetation communities. Geomorphic features identified in the field include active channels, secondary channels with limited or no surface hydrologic connectivity, accretionary bars, backswamps, and natural levees. Vegetation communities include old-growth and younger conifer forest and deciduous forest, mesic wetlands, grasses, xeric vegetation, and beaver meadows (willow carrs). This definition of floodplain heterogeneity can be applied to any floodplain; expands on the metric for floodplain heterogeneity from Graf (2006) and Wohl and Iskin (2019); and is distinct from the metrics of floodplain connectivity (Ward et al., 2002), surface topographic complexity (Scown et al., 2015, 2016a, 2016b) and riparian vegetation (Aguiar et al., 2009) described in other studies.

Our primary objectives are to (a) quantify floodplain spatial heterogeneity for diverse natural floodplains in the United States using multiple heterogeneity metrics from landscape ecology, (b) evaluate whether statistically significant patterns occur among these data and determine whether there are salient characteristics of river corridors that relate to multiple facets of heterogeneity, and (c) interpret the statistical results in terms of the primary

controls—channel lateral mobility and valley-floor space available—as well as the factors underlying mobility and space, such as flow regime and biota. We first review floodplain functions and the importance of floodplain spatial heterogeneity, then present the conceptual model and hypotheses.

1.1. Importance of Floodplain Heterogeneity

Floodplains provide many ecological functions and the services they support (Petsch et al., 2022) including, but not limited to: soil formation, nutrient cycling, primary production, habitat provisioning, water regulation, erosion control, water purification, waste treatment, disease regulation, climate regulation, genetic resources, esthetic, and cultural services. They store material and facilitate the internal and external exchange of surface water, hyporheic water, groundwater, solutes including dissolved carbon, nitrogen and phosphorous, sediment, and organic matter including coarse particulate organic matter and large wood (Appling et al., 2014; Hopkins et al., 2018; Wohl, 2021). Floodplains more effectively capture and biologically process organic matter when compared to laterally confined river reaches with small to no floodplains (Bellmore & Baxter, 2014; Wohl, Lininger, et al., 2018) and store large wood (Iskin & Wohl, 2021). They provide habitat for a diverse array of organisms, including microbes (Bellmore & Baxter, 2014; Benke, 2001; Doering et al., 2021; Jeffres et al., 2008; Tockner et al., 2000; Zeug and Winemiller, 2008) and are commonly more biodiverse than other landcover types (Junk & Piedade, 2010; Tockner et al., 2008). Exchange of water between the river and the floodplain can be similar for both large and small rivers (D. T. Scott et al., 2019), highlighting the importance of studies that incorporate multiple river sizes.

Floodplain heterogeneity both reflects and influences water and sediment connectivity. Fluxes and storage of water and sediment can modify floodplain configuration and alter connectivity, but these fluxes also respond to existing connectivity. Consequently, floodplain connectivity is dynamic in time, changing with the rising and falling limbs of inundating flows (Arscott et al., 2002; Junk et al., 1989; Tockner et al., 2000), as well as in response to channel movement and associated erosion and deposition (Amoros & Bornette, 2002; Stanford et al., 2005), vegetation dynamics (L. G. Larsen & Harvey, 2010; Naiman et al., 2005), movement and storage of large wood (Wohl, 2021), modifications created by other biota (A. Larsen et al., 2021), and disturbances such as wildfire (Kleindl et al., 2015). Increased spatial heterogeneity of the entire river corridor, including floodplain presence, is associated with decreased catchment-wide sediment yield and sediment connectivity (Baartman et al., 2013).

Floodplain heterogeneity also influences floodplain forms and functions. Heterogeneity enhances diversity of hydrologic flow paths within the floodplain and thus diversity of water temperatures, water residence times, and associated biogeochemical reactions (Fuchs et al., 2009; Helton et al., 2014; Uno, 2016). Channel migration that creates heterogeneity also increases floodplain habitat diversity (Choné & Biron, 2016; Stella et al., 2011). Spatial heterogeneity in floodplain soils results in heterogeneity of channel sinuosity and meander migration patterns (Güneralp & Rhoads, 2011; Schwendel et al., 2015). Floodplain heterogeneity affects the deposition and storage of pollutants because many contaminants travel adsorbed to sediment or are influenced by spatially diverse microbial transformations in patchy surface and subsurface environments (Ciszewski & Grygar, 2016; Lowell et al., 2009). Floodplain soil heterogeneity affects carbon and nitrogen cycling (Appling et al., 2014) and carbon storage (Lininger et al., 2018; Samaritani et al., 2011). Surface heterogeneity of vegetation is associated with near-surface soil nutrient heterogeneity (Appling et al., 2014; Naiman et al., 2005). Floodplain topographic heterogeneity influences inundation patterns and resulting vegetation establishment (Friedman & Lee, 2002; Hughes, 1997; M. L. Scott et al., 1996), as well as fish life cycles, aquatic communities, and food webs (Bellmore et al., 2013; Stoffers et al., 2022; Uno et al., 2022; Zeug and Winemiller, 2008). These previous studies highlight the importance and the effects of floodplain heterogeneity, but there is much work to be done in comparing heterogeneity across latitudes, elevations, and biomes and connecting heterogeneity to overarching floodplain processes.

This study builds directly off the development of a classification workflow and choice of metrics from landscape ecology in Iskin (2023) and Iskin and Wohl (2023b), and extends the investigation to floodplain heterogeneity around the continental United States. We move beyond the case study by quantifying floodplain spatial heterogeneity for 15 natural floodplains across North America that differ in relative channel mobility, flashiness of flood peaks, and biome to provide insights into the fluvial and ecological processes that create and maintain natural floodplain heterogeneity.

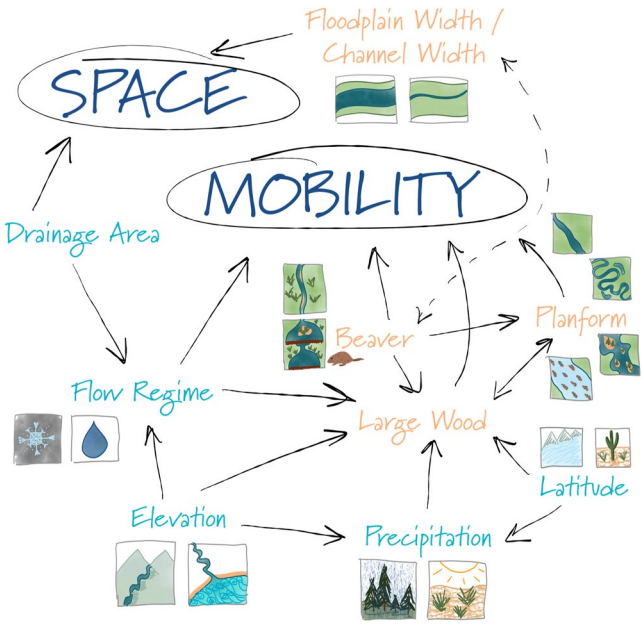

Figure 1. Main controls of floodplain spatial heterogeneity and the predictor variables used to quantify them. Main controls are shown in dark blue text and predictors are shown in turquoise and orange text. Turquoise predictors indicate drainage basin-level values and categories, and orange predictors indicate study area-level values and categories. Solid arrows connect predictor variables to the main controls they represent and to other predictor variables that they influence or are influenced by, and double-sided arrows connect predictor variables the interact reciprocally with each other. The dashed arrow connecting Beaver and Floodplain Width/Channel Width represents the habitat preference of beaver for wider floodplains, but also the fact that beaver presence and dam building can increase the regularly flooded width of the valley floor (e.g., Westbrook et al., 2011). The inset tiles illustrate contrasting values or levels for each variable.

1.2. Conceptual Model

We seek to determine whether river corridor characteristics can predict levels of floodplain heterogeneity through a multivariate linear analysis and to infer processes that create and maintain floodplain heterogeneity. We start from the premise that the two primary controls of floodplain heterogeneity are the lateral space available for floodplain development in a river corridor and the lateral mobility of the channel. For the conceptual model in Figure 1, we assume that the space available for a river is governed primarily by processes acting at timespans of millennia and longer (e.g., Wohl, 2015) and is thus static for the timespans of 10^1–10^2 years during which the floodplain features that we analyze are created and maintained. We use valley geometry to represent valley-floor space available for floodplain development and adjustment based on the erosional and depositional powers of the river relative to erosional resistance of the adjacent uplands. We quantify drainage area and the ratio of average floodplain width to average channel width at the reach scale and use these as indicators of valley geometry because valley-floor width tends to increase with drainage area (e.g., Beighley & Gummadi, 2011; Bhowmik, 1984) but reach-scale variations in longitudinal trends are better captured by floodplain/channel width for a reach (e.g., Wohl et al., 2017).

We expect watershed-scale flow regime, reach-scale channel planform, and regional biota to influence lateral channel mobility. We categorize flow regime in snow and rain and use it as a proxy for the flashiness and relative erosional power of peak flows, assuming that snowmelt-dominated flow regimes are less flashy than rainfall-dominated regimes. Thirty-year normal precipitation is a variable that can be easily quantified from publicly available data and that may influence flow regime and floodplain vegetation. Mean floodplain elevation can be a proxy for elevational differences in climate and disturbance regime, particularly in high-relief watersheds (Sutfin & Wohl, 2019). Categorical planform reflects relative lateral mobility, which we interpret to increase along a continuum from straight to meandering, anastomosing, and then braided channel planforms (Schumm, 1985). Latitude and elevation are likely to jointly distinguish ecoregions in the United States (Barry et al., 2004; Omernik, 1987) and median large wood volume (LWV) reflects a biotic influence on floodplain process and form (Collins et al., 2012) (Figure 1). Methods used to determine values and categories for each predictor variable are described in the Methods section and provided for each site in Table 2.

We relate the predictor variables in Figure 1 to five response variables that are commonly used patch- and class-based heterogeneity metrics from landscape ecology: aggregation index, percentage of like adjacencies (adjacencies), interspersion and juxtaposition index (interspersion), patch density (density), and Shannon's evenness index (evenness) (levels of each metric demonstrated in Figure S1 in Supporting Information S1). Aggregation and adjacencies are both measures of the class clumping across a landscape based on class edge length (He et al., 2000; Hesselbarth et al., 2022). Going forward the term aggregation will be used when we refer to these metrics together. Low values of aggregation indicate that few pixels are adjacent to pixels of the same class (He et al., 2000; Hesselbarth et al., 2022). Interspersion is a measure of intermixing of class types at a patch level, or how spatially mixed patches of different classes are (Hesselbarth et al., 2022; McGarigal & Marks, 1995). Density is a measure of how broken up a landscape is: a higher density indicates a landscape with more individual patches, regardless of class (Hesselbarth et al., 2022). Evenness is a measure of diversity and distribution of classes across a landscape (Hesselbarth et al., 2022). Higher evenness indicates that the landscape is not dominated by one class (McGarigal & Marks, 1995).

1.3. Hypotheses

We test four hypotheses regarding relationships between predictor and response variables using pairwise comparisons of medians and variances, and a multivariate linear analysis.

Hypothesis 1. **(H1)**: Aggregation will increase and density will decrease with increasing floodplain/channel width. We based this hypothesis on the assumption that the turnover rate of a relatively broad floodplain will be longer (Konrad, 2012; Mertes et al., 1996) and individual patches will persist for longer and be subject to less frequent disturbance, thus merging into larger patches via vegetation establishment and encroachment.

Hypothesis 2. **(H2)**: Aggregation, interspersion, density, and evenness will increase with increasing large wood volume. This tests the inference that large wood accumulations can increase channel-floodplain connectivity (Collins et al., 2012; Jeffries et al., 2003), increasing the size of patches, but can also affect vegetation establishment, store sediment, and armor channel banks (Daniels & Rhoads, 2003; Skalak & Pizzuto, 2010).

Hypothesis 3. **(H3)**: For non-beaver sites, interspersion, evenness, and density will increase and aggregation will decrease with increasing channel mobility and migration (as reflected in the proxy of planform). This hypothesis tests the assumption that new floodplain will be formed, vegetation succession will be reset, and sediment will be transported and deposited in new areas, thus dissecting large patches and therefore increasing the number of patches and class intermixing.

Hypothesis 4. **(H4)**: Interspersion, evenness, and density will increase and aggregation will decrease with increasing flow regime flashiness (as reflected in the category of flow regime). This hypothesis tests the inference that the channel will be more mobile, and the floodplain will be inundated more often with less time for large vegetation to establish (e.g., Everitt, 1968), increasing the number of small, interspersed patches and dissecting large patches.

2. Study Area

We chose 15 diverse river corridors from the continental United States (Figure 2; Table 2) to represent a range of drainage area (30–500,000 km^2), flow regime (snowmelt vs. rainfall), channel planform (straight, meandering, anastomosing, beaver, braided), and biome/latitude (31–66°). We selected the least human-altered floodplains and watersheds that we could identify to minimize the effects of flow regulation, artificial levees, floodplain drainage and land cover changes, and channel engineering on floodplain process and form.

3. Methods

Following the methods from Iskin (2023) and Iskin and Wohl (2023b), we present a full suite of sites with field data and classified floodplains with quantified spatial heterogeneity and employ statistical methods to investigate relationships between river corridor characteristics and floodplain heterogeneity. Data were collected at the study reaches along transects. Study reaches were chosen based on existence of a floodplain (river beads), access by car and foot, and in some cases by existence of published data sets. Field transect locations were spaced at approximately 10 times the average channel width. Classes were identified in the field based on geomorphic, hydrologic, and vegetation features. Patch were delineated along the floodplain transects on the 3–10 m scale and their boundaries were collected with a Garmin GPSMAP 66ST handheld GPS (±3 m horizontal accuracy). Field classifications for specific sites can be found in Table S1 in Supporting Information S1, Iskin and Wohl (2023b), Table 3, and Iskin (2023), Table 3.1.

Large wood (≥10 cm diameter, ≥1 m length) locations and diameters were collected along the transects. Large wood loads (volume) were then calculated from field transect data and from various sources that generally coincide with the delineated floodplains (Table 1) according to Van Wagner's method (1968) using mapped transect length (Figure 3). Large wood volume estimates represent minima for some sites because we could not access the channel or floodplain on both sides of the channel (Iskin, 2023).

Two types of remote data were compiled: (a) remote imagery and (b) watershed and reach characteristics. Google Earth Engine (Gorelick et al., 2017) was used to create 2022 cloud-free mosaics of Copernicus Sentinel-2A 10- and 20-m bands coinciding with each floodplain. Lidar-derived digital elevation models (DEMs) were obtained from various sources. The highest spatial resolution publicly-available DEMs that covered the study sites were used. Specifics on Sentinel and DEM data collection can be found in Text S2 in Supporting Information S1 and Table S2 in Supporting Information S1.

Site variables were also compiled for each site: latitude and longitude, drainage area, floodplain area, floodplain perimeter, mean floodplain elevation (elevation), annual average precipitation (precipitation), categorical flow

10.1029/2023WR035162

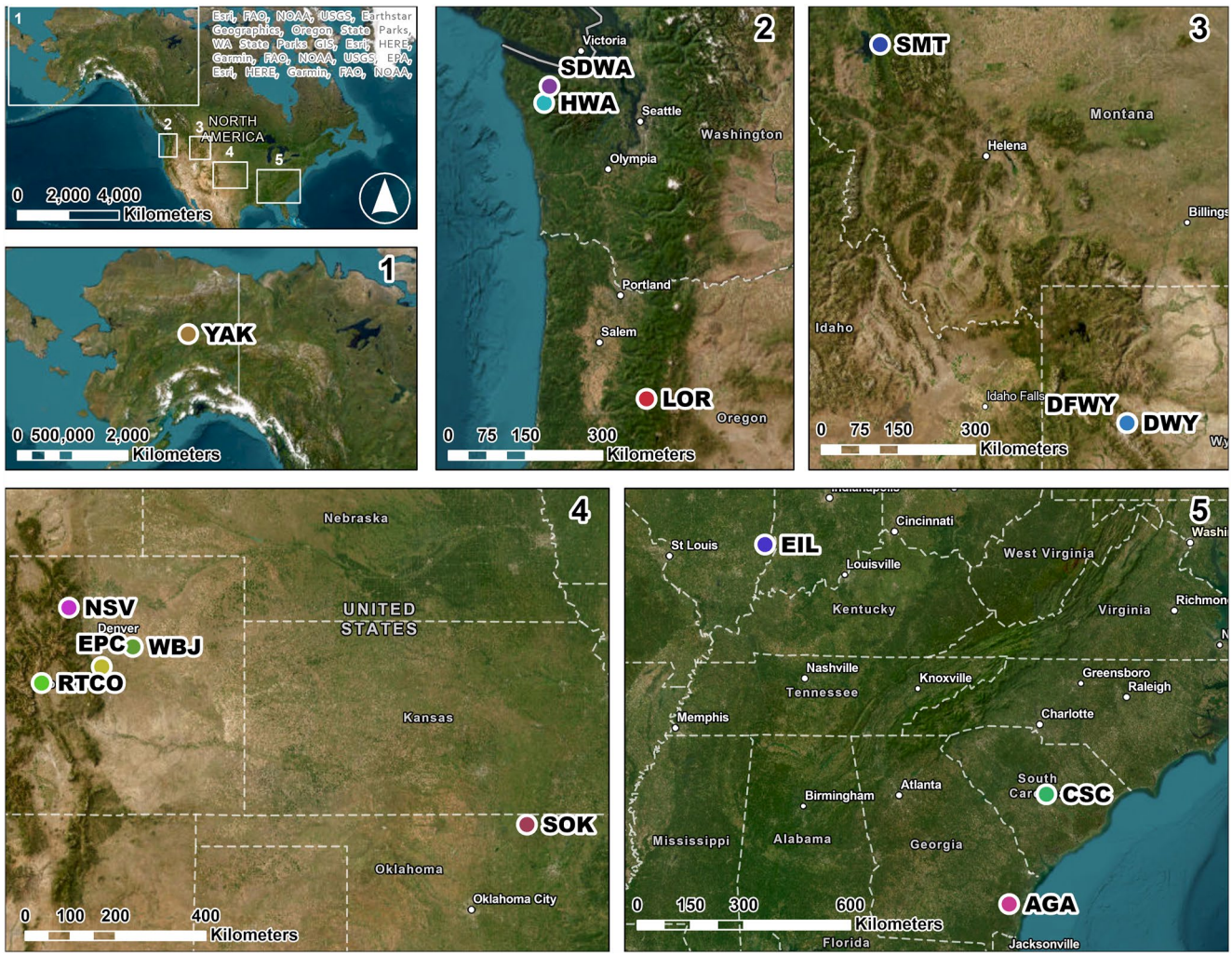

Figure 2. Floodplain sites used in this study, shown regionally and in more detail. Region 1 includes the Yukon River in the arctic (YAK); region 2 includes the Hoh River (HWA), Sol Duc River (SDWA), and Lookout Creek (LOR) in the Pacific Northwest; region 3 includes the Swan River (SMT), Downs Fork (DFWY), and Dinwoody Creek (DWY) in the Rocky Mountains; region 4 includes North St. Vrain Creek (NSV), Rough and Tumbling Creek (RTCO), East Plum Creek (EPC), West Bijou Creek (WBJ), and Sand Creek (SOK) in the Rocky Mountains and Great Plains; and region 5 includes Embarras River (EIL), Congaree River (CSC), and Altamaha River (AGA) in the (coastal) plains.

regime, categorical planform, total sinuosity, and ratio of average floodplain width to average channel width (floodplain width ratio) (Table 2).

Drainage areas were obtained using StreamStats (USGS, 2023b) to delineate the contributing areas upstream of the study reaches (Table S2 in Supporting Information S1), with the pour points specified as the downstream-most parts of the study reaches. The basin polygons were brought into ArcGIS Pro (Esri, 2022) and the geodesic areas were calculated using *Calculate Geometry*. StreamStats is not available for interior Alaska or the State of Wyoming, so the drainage basins for the Yukon, Dinwoody Creek, and Downs Fork were delineated in ArcGIS Pro using the *Watersheds (Ready to Use)* tool (Esri, 2023) with the default snap distance and finest data source resolution (Table S2 in Supporting Information S1). Latitude and longitude were obtained from the pour points used to delineate the watersheds.

Floodplain boundaries were delineated manually in ArcGIS Pro using field transect data, Sentinel imagery, DEMs, and national park boundaries (where applicable). A 10-m geodesic buffer was added to the floodplains to account for field and/or user error (Iskin & Wohl, 2023b). Additional specifics on floodplain delineation can be found in Text S2 in Supporting Information S1. Floodplain area and perimeter were obtained by calculating the geodesic areas and perimeters from the floodplain polygons. The Sentinel and DEM images were clipped to the buffered floodplain polygons, and mean floodplain elevations were acquired from the clipped DEM statistics.

Table 1
Floodplain Large Wood Loads for the United States

River	Median transect wood load (m^3/ha)	Range (m^3/ha)	Number of transects	Collected
Yukon River[a]	30	0–170	24 (patches)	June and July 2015
Altamaha River	10	0–140	4	October 2021
Congaree River[b]	50	1–180	NA	October and November 2009
Embarras River	1,120	140–2,220	4	March 2022
Swan River[c]	140	130–150	16	July 2017
West Bijou Creek	130	20–220	10	July and October 2020
Hoh River	2,760	140–8,820	7	July 2021
East Plum Creek	0	No wood observed	3	September 2020
Dinwoody Creek	20	20–30	5	July 2019
Sol Duc River	3,900	800–18,900	10	July 2021
North St. Vrain Creek[d]	0	No wood observed	10	August 2010 and August 2018
Downs Fork	30	10–50	6	July 2019
Rough and Tumbling Creek	0	No wood observed	1	August 2022
Lookout Creek	4,110	0–8,660	10	July 2022
Sand Creek	0	0–600	10	June 2021

Note. These estimates include some instream wood at sites where the active channel was accessible by foot. Values are rounded to the nearest ten.
[a]Lininger et al. (2017) (Note: wood volumes do not include wood jams that were on the channel margins). [b]Wohl et al. (2011). [c]Wohl, Scott, et al. (2018). [d]Laurel and Wohl (2019) and Wohl and Cadol (2011).

Precipitation values were obtained from modeled average annual precipitation data for the coterminous U.S. (800 m resolution, 1991–2020 time period; PRISM, 2022), Alaska (800 m resolution, 1991–2020 time period; PRISM, 2018), and western Canada (2 km resolution, 1961–1990 time period; PRISM, 2002). The data were clipped to the respective drainage areas, and the mean values in millimeters were extracted from the raster statistics. Flow regime was determined from visual inspection of 2021–2023 annual gauge/discharge data for each site, and from nearby sites for ungauged streams (USGS, 2023a). A snowmelt-dominated flow regime was assigned when the annual discharge had a few-months-long peak in the late spring/early summer, and a rainfall-dominated flow regime was assigned when the annual discharge had many short peaks in the year.

Planform classifications reflect a continuum based on flow, sediment, and wood regimes (Schumm, 1985), but we chose one planform category for each site (straight, meandering, anastomosing, beaver, or braided) based on field observations. We also calculated total sinuosity using base-flow imagery for each site available in Google Earth Pro as of March 2023 as a less subjective and numerical measure of planform characteristics. Average floodplain/channel width was calculated in ArcGIS Pro by measuring manually delineated floodplain widths and channel widths. Floodplain widths were measured perpendicular to the valley trend using the floodplain polygons. Channel widths were measured perpendicular to flow direction at the same locations as the floodplain widths using the Sentinel satellite imagery, DEMs, and ArcGIS Pro National Agriculture Imagery Program Hybrid base map where necessary (Iskin, 2023).

3.1. Analysis

Classification of the 15 study floodplains followed a similar workflow to Iskin (2023) and Iskin and Wohl (2023b) and is detailed in Figure 3. Classes are identified on the 10-m scale with an unsupervised remote sensing classification run on a stack of data containing the Sentinel imagery, DEMs, and normalized difference vegetation index and normalized difference moisture index created using bands from the Sentinel imagery (Table S2 in Supporting Information S1), as described in greater detail in Text S2 in Supporting Information S1. An unsupervised classification scheme was used because the class types varied greatly across the US, and we did not want to limit the classifier to only finding the classes we saw in the field (e.g., with a supervised classification). We assume that

10.1029/2023WR035162

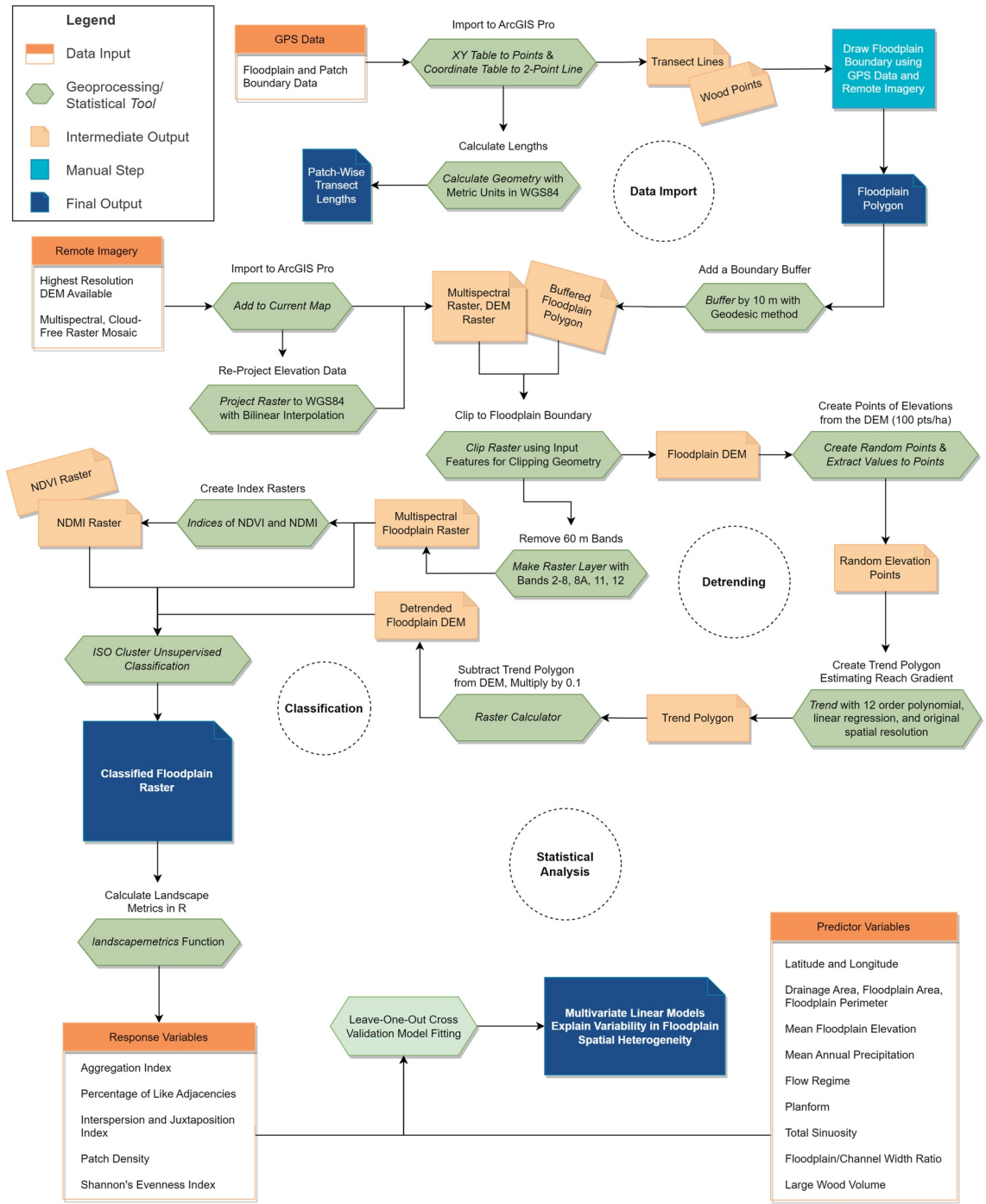

Figure 3. Analytical workflow completed in ArcGIS Pro and RStudio.

the metrics calculated from the classification are not very sensitive to the specific area that is being classified. For example, we assume that adding the 10-m buffer will not significantly affect the results.

The classified floodplains and the data from Tables 1 and 2 were brought into R (R Core Team, 2023) and prepared for analysis and visualized using tools from the *tidyverse*, *raster*, *rasterVis*, and *rgdal* packages (Bivand et al., 2023; Hijmans, 2023; Lamigueiro & Hijmans, 2023; Wickham et al., 2019). The heterogeneity metrics of aggregation index (aggregation), percentage of like adjacencies (adjacencies), interspersion and juxtaposition index (interspersion), patch density (density), and Shannon's evenness index (evenness) described earlier were calculated using the *landscapemetrics* package (Hesselbarth et al., 2019).

Water Resources Research

10.1029/2023WR035162

Table 2
Predictor Variables and Sources

River	Latitude	Longitude	Drainage area	Floodplain area	Floodplain perimeter	Elevation	Precipitation	Flow Regime	Planform	Sinuosity	Width ratio
Units	DD	DD	km^2	km^2	km	m	mm	–	–	m/m	m/m
Yukon River	65.9	−149.2	500,329	2,378.2	401.8	110	438	Snow	Anastomosing	13.3	7.5
Altamaha River	31.4	−81.6	36,542	37.1	32.2	1	1,233	Rain	Straight	1.2	19.3
Congaree River	33.8	−80.7	21,918	106.1	53.8	30	1,248	Rain	Meandering	2	59.2
Embarras River	38.9	−87.8	5,496	6.2	21	130	1,098	Rain	Meandering	2.2	25.9
Swan River	47.9	−113.9	1,540	26.2	65.2	960	1,062	Snow	Anastomosing	4.8	12.5
West Bijou Creek	39.6	−104.3	653	1.1	6.5	1,630	459	Rain	Braided	2.2	4.1
Hoh River	47.8	−124	323	9.9	19	160	3,984	Rain	Braided	4.1	7
East Plum Creek	39.3	−104.9	192	0.02	0.6	1,950	552	Snow	Straight	1.3	19.4
Dinwoody Creek	43.3	−109.6	131	0.3	3.2	2,810	834	Snow	Meandering	1.6	14.3
Sol Duc River	48	−123.9	101	0.6	6.1	420	3,856	Rain	Meandering	1.5	7
North St. Vrain Creek	40.2	−105.5	84	0.4	3.5	2,540	935	Snow	Beaver	2.6	13.7
Downs Fork	43.3	−109.6	62	0.2	2.2	2,810	849	Snow	Anastomosing	5.6	17
Rough and Tumbling Creek	39.1	−106.1	60	0.1	1.1	2,950	591	Snow	Beaver	2.6	8.1
Lookout Creek	44.2	−122.2	54	0.1	2.1	540	2,341	Rain	Straight	1.3	3.2
Sand Creek	36.8	−96.4	31	0.1	2.2	300	994	Rain	Meandering	1.5	2.8
Scale		*Drainage Area*			*Study Reach*		*Drainage Area*	*Regional*		*Study Reach*	

Note. Latitude, longitude, floodplain area, floodplain perimeter, total sinuosity, and floodplain-channel width ratio are rounded to the nearest tenth; drainage area and precipitation are rounded to the nearest one; and elevation is rounded to the nearest ten.

The continuous predictor variables of latitude, longitude, drainage area, floodplain area, floodplain perimeter, elevation, precipitation, total sinuosity, and floodplain width ratio are compared to the calculated heterogeneity metrics via correlation. The categorical predictor variables are compared to the heterogeneity metrics using boxplots and non-parametric comparisons of medians using the *coin* and *dunn.test* packages (Dinno, 2017; Hothorn et al., 2008), and variances using the *car* package (Fox & Weisberg, 2019). For the analysis, flow regime was ordered by flashiness (Snow < Rain) and planform was ordered by channel mobility (Straight < Meandering < Anastomosing < Beaver < Braided). Multivariate linear models are fit using the *lm* function, and the nonparametric method of leave-one-out cross-validation (LOOCV) is used to choose the most appropriate models using the *tidymodels* package (Kuhn & Wickham, 2020). Five models are fit with each heterogeneity metric as the response variable. The LOOCV model selection is iterative and is ultimately based on choosing the model with the highest LOOCV R^2 value.

4. Results

The 15 classified floodplains are presented in Figure 4 and through a quantitative comparison of the heterogeneity metrics for each floodplain. Correlations and pairwise comparisons of heterogeneity between the levels of the categorical variables are provided, and the LOOCV multivariate models are presented. H1–H4 are discussed first with qualitative results and then with the model results. To summarize the results, floodplain heterogeneity is significantly related to river corridor characteristics and some heterogeneity metrics are also significantly related to each other.

4.1. Classification

The classified floodplains for all sites are provided in Figure 4. Detail insets are provided for floodplains with an area ≥10 km^2. The Yukon River floodplain is the largest floodplain in this study (>2,000 km^2) and spans nine DEM tiles from three different years (Table 2, Table S2 in Supporting Information S1).

4.2. Exploratory Statistics

The overall median values of floodplain heterogeneity as quantified by five metrics are presented in Table 3. These results indicate that natural floodplains have moderate aggregation of classes, high evenness and intermixing of classes, and a wide range of patch densities.

Some of the heterogeneity metrics demonstrate high collinearity with each other, as shown in fitted linear models in Equations 1–3 and pairwise scatter plots in Figure S2 in Supporting Information S1 (bold values in the equations represent p-values <0.05 for the models and individual predictors). The results show that adjacencies describes 97% of the variability in aggregation, indicating that perhaps only one of these metrics is necessary to capture the level of aggregation in a landscape. The opposite relationship between the aggregation metrics and density makes intuitive sense as one would expect an increase in the number of patches to decrease class aggregation (Equations 1 and 3). Because aggregation and adjacencies are highly correlated, aggregation will be the only aggregation metric discussed going forward.

$$\text{Aggregation Index} = \mathbf{-0.018} \times \mathbf{\text{Patch Density}} + \mathbf{83.00};\ \text{Multiple } R^2 = \mathbf{0.88} \quad (1)$$

$$\text{Aggregation Index} = \mathbf{1.04} \times \mathbf{\text{Adjacencies}} - 1.54;\ \text{Multiple } R^2 = \mathbf{0.97} \quad (2)$$

$$\text{Patch Density} = \mathbf{-49.97} \times \mathbf{\text{Adjacencies}} + \mathbf{4226.34};\ \text{Multiple } R^2 = \mathbf{0.84} \quad (3)$$

Correlation tables were calculated for all the predictor and response variables (n = 15) (Table S3 in Supporting Information S1) to examine numerical relationships. There is some collinearity in the set of predictor variables, particularly latitude, longitude, floodplain area and perimeter, and total sinuosity. This intuitively makes sense as the variables are interconnected (Figure 1). Because of this, we removed latitude, longitude, and floodplain area and perimeter to obtain a final suite of predictor variables of drainage area, elevation, precipitation, total sinuosity, LWV, floodplain/channel width ratio, flow, and planform. We kept total sinuosity because it is the only numerical indicator of channel planform. The correlations (Table S3 in Supporting Information S1) show that floodplain/channel width is weakly negatively correlated with aggregation, not supporting H1. Large wood

10.1029/2023WR035162

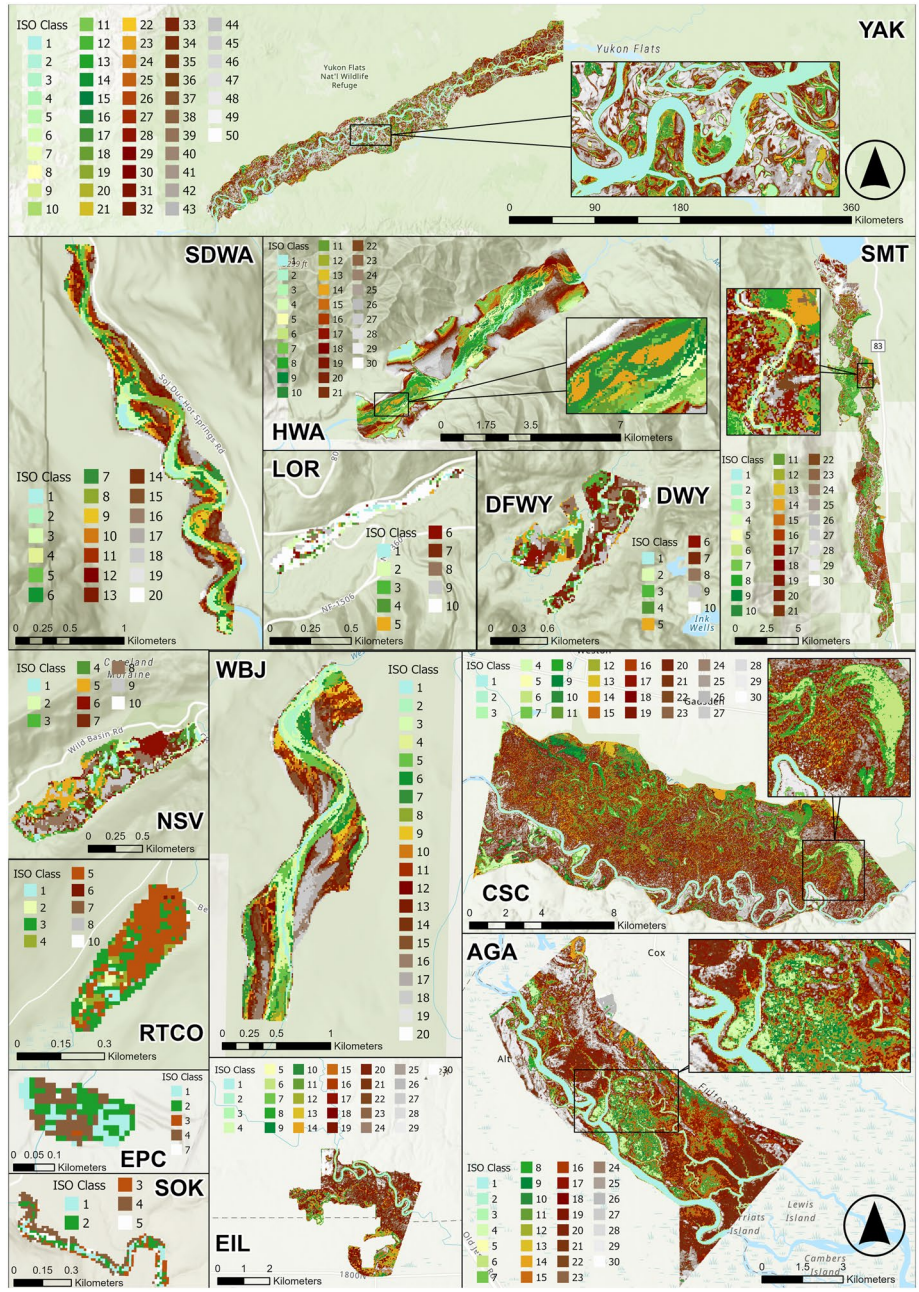

Figure 4. Unsupervised classification (ISO) results for Regions 1–5: Yukon River, Alaska (YAK; with detail inset); Sol Duc River, Washington (SDWA); Hoh River, Washington (HWA; with detail inset); Swan River, Montana (SMT; with detail inset); Lookout Creek, Oregon (LOR); Downs Fork, Wyoming (DFWY); Dinwoody Creek, Wyoming (DWY); North St. Vrain Creek, Colorado (NSV); Rough and Tumbling Creek, Colorado (RTCO); West Bijou Creek, Colorado (WBJ); East Plum Creek, Colorado (EPC); Sand Creek, Oklahoma (SOK); Embarras River, Illinois (EIL); Congaree River, South Carolina (CSC; with detail inset); and Altamaha River, Georgia (AGA; with detail inset). ISO classes are not equal to field classes.

volume is weakly negatively correlated with aggregation and evenness, and weakly positively correlated with density, partially supporting H2. Drainage area is strongly positively correlated with aggregation, weakly positively correlated with evenness, and strongly negatively correlated with density. Precipitation is weakly positively correlated with density and evenness, and weakly negatively correlated with aggregation. Total sinuosity follows the same trends as drainage area, partially supporting H3. This makes sense as these two predictor variables are strongly positively correlated. Elevation is weakly negatively correlated with evenness, density, and interspersion, and weakly positively correlated with aggregation.

Table 3
Calculated Heterogeneity Metrics for Each Site

River	Aggregation (%)	Interspersion (%)	Density (patches/100 ha)	Adjacencies (%)	Evenness
Yukon River	75.7	73.4	491	75.6	0.966
Altamaha River	58.8	73.3	1,213	58.5	0.934
Congaree River	52.3	73.2	1,578	52.1	0.922
Embarras River	55.7	71.7	1,335	55.2	0.906
Swan River	50.8	78.9	1,819	50.6	0.962
West Bijou Creek	56.7	80.2	1,328	55.4	0.973
Hoh River	66.0	71.6	855	65.3	0.973
East Plum Creek	60.6	55.2	1,168	56.7	0.721
Dinwoody Creek	60.2	79.3	1,217	58.9	0.917
Sol Duc River	50.8	79.9	1,866	49.5	0.967
North St. Vrain Creek	61.4	83.4	1,148	60.1	0.957
Downs Fork	69.5	78.3	832	67.0	0.927
Rough and Tumbling Creek	65.8	55.8	1,241	64.1	0.554
Lookout Creek	57.4	74.9	1,698	58.6	0.639
Sand Creek	46.9	96.6	1,823	48.6	0.972
Median	**58.8**	**74.9**	**1,241**	**58.5**	**0.934**

Note. Color scales represent red = 25%, yellow = 50%, and green = 75% of the metric's range, excluding density. The patch density color scale represents red = lowest value, yellow = 50th percentile, and green = highest value. Aggregation, interspersion, and adjacencies are rounded to the nearest tenth, density is rounded to the nearest one, and evenness is rounded to the nearest hundredth.

Comparing median heterogeneity values among the categorical variables of planform (Figure 5) and flow regime (Figure 6) show that there are no significant differences in medians (Wilcoxon Rank Sum, Wilcoxon Rank Sum with ties, and Kruskal-Wallis Rank Sum test p-values all >0.05). There are also no significant differences in variances by flow regime (Levene's test p-values >0.05), but there are significant differences in variances for evenness by planform (Levene's test p-values <0.05).

Although there are no significant differences in medians, we can draw qualitative inferences in relation to the conceptual model-based hypotheses (H3–H4). H3 proposed that interspersion, evenness and density would increase with increasing channel mobility. Figure 5b shows that straight planforms (least mobile) generally have lower interspersion than the other planform types, supporting H3. Figure 5c shows that meandering planforms have greater density than straight planforms, but that anastomosing and braided planforms (most mobile) have lower density than all the others, partially supporting H3. Figure 5d shows that median evenness increases from least mobile to most mobile planforms, supporting H3. H3 also proposed that aggregation would decrease with channel mobility. From Figure 5a, meandering planforms have the lowest aggregation and straight, anastomosing, and braided planforms have similar and higher aggregation. This only partially supports H3, as straight planforms have higher aggregation than meandering, but anastomosing and braided planforms also have greater aggregation than meandering. Overall, H3 is primarily supported by the data, but inclusion of more sites in each planform category would strengthen future analyses.

Similar to H3, H4 proposed that interspersion, evenness and density would increase and aggregation would decrease with increasing flow regime flashiness. Figures 6b and 6d show that median interspersion and evenness are similar for snowmelt (less flashy) and rainfall (flashier) flow regimes, not supporting H4. Figure 6c, however, shows increasing density with increasing flashiness of the flow regime, supporting H4. Figure 6a shows that aggregation decreases with increasing flashiness, supporting H4. Overall, we conclude that H4 is partially supported by the data.

4.3. Multivariate Models

Multiple attempts using standard methods for multivariate linear analysis led to overfitting and little applicability beyond the data set of 15 sites. Instead, we used a non-parametric method of model fitting that guards against

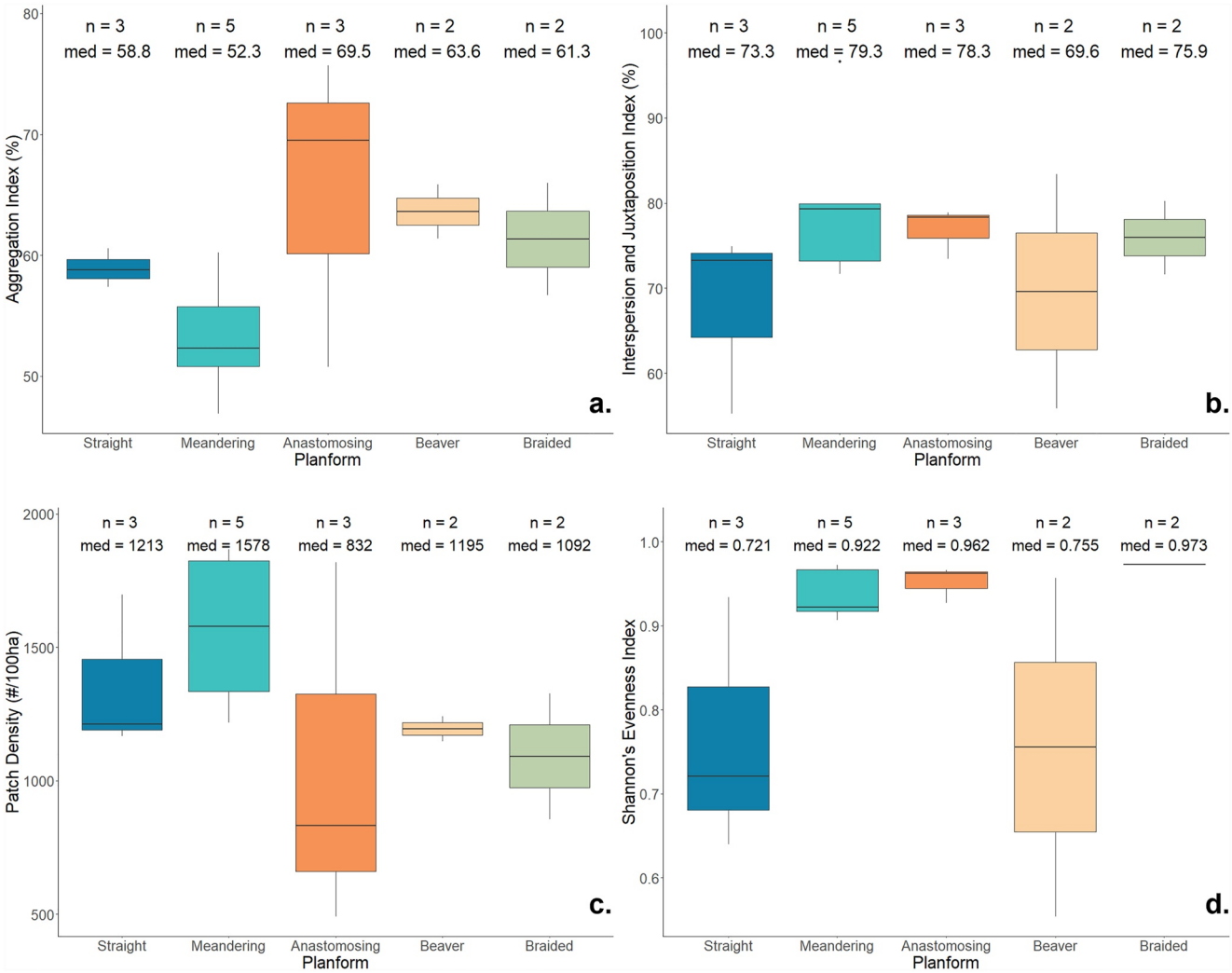

Figure 5. Pairwise comparisons of heterogeneity metrics by reach-scale channel planform for (a) aggregation, (b) interspersion, (c) density, and (d) evenness. There are no statistical differences in medians.

overfitting and can provide insights into important predictors of floodplain heterogeneity. The final LOOCV models are presented in Table 4. Boxplots of the estimates for each predictor variable for each model are given in Figures S3–S6 in Supporting Information S1. Predictor values are considered "important" (as opposed to statistically significant) if the interquartile range of the boxplots does not include zero and the range of the boxplots are reasonably narrow.

The results show that 45% of the variability in aggregation can be explained by the full model. Drainage area, elevation, floodplain/channel width, planform, and flow regime are important in this model, with smaller drainage areas, higher elevations, and greater floodplain width ratios corresponding to larger aggregation values, supporting H1. Straight planforms have higher aggregation than anastomosing, beaver, and braided planforms, partially supporting H3. Rainfall-dominated flow regimes have higher aggregation than snowmelt-dominated, not supporting H4. Large wood volume can explain 77% of the variability in interspersion. The combination of drainage area, total sinuosity, LWV, and planform can explain 48% of the variability in density. All these predictor variables are important in this model, with larger drainage areas, higher large wood volumes, and lower total sinuosity corresponding to larger density values, supporting H2. Straight planforms have lower density than anastomosing and braided planforms, supporting H3. Lastly, precipitation can explain 59% of the variability in evenness and is important in this model, with greater annual average precipitation over the drainage area corresponding with an increase in evenness. Table 5 summarizes support of Hypotheses H1–H4 from the qualitative and quantitative results.

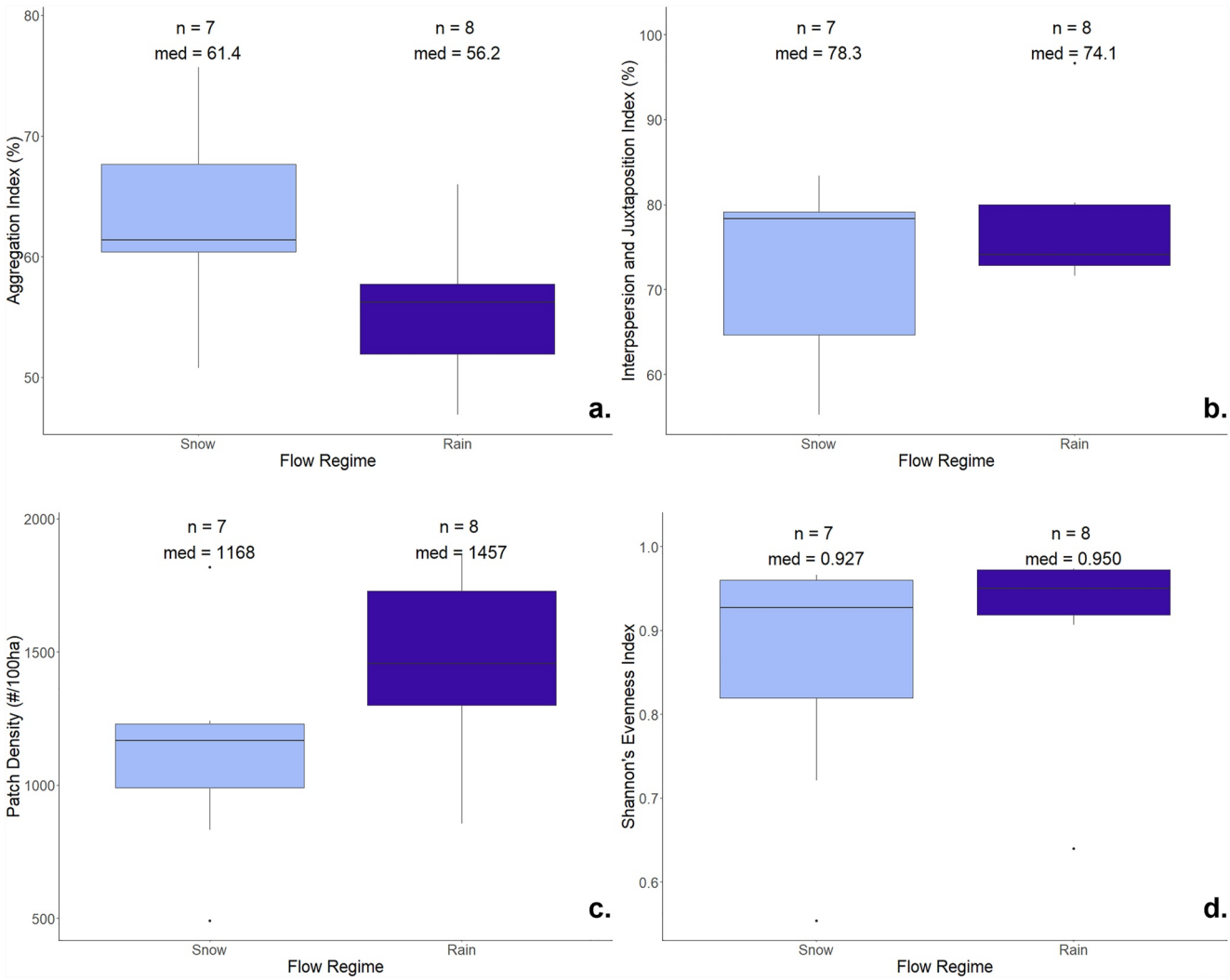

Figure 6. Pairwise comparisons of heterogeneity metrics by watershed-scale flow regime for (a) aggregation, (b) interspersion, (c) density, and (d) evenness. There are no statistical differences in medians.

5. Discussion

The main controls of floodplain spatial heterogeneity are the space a river has available and the mobility of the channel across its floodplain (Figure 1). The predictor variables were chosen specifically to capture different fluvial processes that relate to and affect space and mobility. Determining the specific controls of floodplain heterogeneity within channel mobility and space available is complex, especially with a small sample size. The

Table 4
Leave-One-Out Cross-Validation Multivariate Models and R^2 Values

Response variable	Predictor variables	LOOCV R^2
Aggregation	DrA + Elev + Precip + TS + LWV + FP/CH + Plan + Flow	0.45
Interspersion	LWV	0.77
Density	DrA + TS + LWV + Plan	0.48
Evenness	Precip	0.59

Note. Drainage area (DrA), mean floodplain elevation (Elev), annual average precipitation (Precip), total sinuosity (TS), large wood volume (LWV), ratio of average floodplain width to average channel width (FP/CH), categorical planform (Plan), and categorical flow regime (Flow) emerge as important predictor variables.

Table 5
Summary of Support for Study Hypotheses

Hypothesis	Result
H1: ↑ in aggregation, ↓ in density with ↑ in floodplain/channel width	Partially Supported
H2: ↑ in aggregation, interspersion, density, evenness with ↑ large wood volume	Supported
H3: ↑ in interspersion, density, evenness, ↓ in aggregation with ↑ mobility	Supported
H4: ↑ in interspersion, density, evenness, ↓ in aggregation with ↑ flashiness	Partially Supported

non-statistically significant boxplot comparisons show that there may be differences in heterogeneity between planform and flow regime types, but the low sample sizes at the individual levels of the categorical variables are probably obscuring potential differences. The main takeaways from the exploratory analysis are (a) the general trends seen across sites of moderate aggregation, high interspersion and evenness, and varying patch density and (b) the potential for large wood in the river corridor to significantly influence floodplain spatial heterogeneity in a greater diversity of rivers than documented in previous studies. Future work could focus on establishing thresholds for these metrics, such as between planform types of natural floodplains and for natural versus degraded floodplains.

A sample size of 15 is small in the realm of statistics but these data points reflect substantial time and effort and both the qualitative and LOOCV analyses provide a launching point for future study. More work could be done to (a) identify a more robust way to choose the maximum number of classes in the unsupervised classification workflow, as it is known that these metrics are sensitive to the number of classes used (Huang et al., 2006), and (b) test whether the delineated floodplain area significantly affects the metrics. Ways to reduce discrepancies in the satellite data could be further investigated as well. However, the results from the classification workflow are straightforward and are discussed at length in Iskin (2023) and Iskin and Wohl (2023b), so the following discussion addresses both the qualitative results from the boxplot comparisons and quantitative results from the LOOCV model fitting. Qualitatively, H2 and H3 are supported and H1 and H4 are partially supported. Quantitatively, river corridor characteristics can explain 45%–77% of the variability in floodplain heterogeneity, providing insights into the fluvial processes that create and maintain floodplain heterogeneity. An important caveat on this discussion is that some variables potentially relevant to channel lateral mobility and thus floodplain spatial heterogeneity, such as discharge, sediment load in the channel (Constantine et al., 2014), or floodplain stratigraphy (Güneralp & Rhoads, 2011), were not quantified in this study.

Shifting focus to the quantitative results, drainage area, elevation, precipitation, total sinuosity, LWV, floodplain/channel width ratio, planform, and flow regime type all influence floodplain heterogeneity. This supports the idea that heterogeneity is complex and reflects the influence of many fluvial processes. Additionally, no model is the same (Table 4), indicating that the heterogeneity metrics are capturing difference facets of floodplains heterogeneity and that it may be important to consider all four metrics when assessing a floodplain's heterogeneity across space and through time.

We infer that channel mobility in the form of planform and total sinuosity influences floodplain heterogeneity, and that there is (a) a difference in aggregation between straight and all other planforms, (b) a difference in density between straight and the most mobile planforms (anastomosing and braided), and (c) that patch density decreases with increasing total sinuosity. This is an interesting result as we would expect increasing channel mobility (straight < meandering < anastomosing < braided) to be positively related to increasing total sinuosity (Hong & Davies, 1979), but we see the opposite trend with density, a pattern that remains to be explained. Channel planform reflects differences in rates and styles of lateral mobility and associated patchiness of the floodplain. Meandering channels, for example, move in predictable directions, with meander migration toward the outside of each bend and episodic cutoffs. Braided channels are more likely to experience avulsion (e.g., Ashmore, 2009) rather than gradual lateral migration and to create a three-dimensional mosaic of floodplain topography and stratigraphy rather than the meander-scroll topography and fining upward stratigraphy characteristic of meandering rivers (Miall, 1997). Previous studies suggest that channel planform integrates the effects of flow regime, sediment dynamics, large wood load, and floodplain vegetation, so it makes sense that channel planform is an important factor influencing reach-scale floodplain heterogeneity in this analysis. This study adds to that understanding by examining correlations among these variables and floodplain heterogeneity across diverse river systems. To

return to the conceptual model, channel planform reflects differences in lateral mobility and space available in that braided, anastomosing, and meandering channels require a greater minimum floodplain width to develop when compared to straight channels.

We also infer that space available in the form of drainage area and floodplain/channel width ratio exerts an influence on floodplain heterogeneity, and that (a) aggregation decreases with increasing drainage area, (b) aggregation increases with floodplain width ratio, and (c) patch density increases with drainage area. Once again, this is an interesting result as drainage area and floodplain width ratio exhibit opposite trends in relation to aggregation. This supports previous studies that show that reach-scale variations in valley-floor width and floodplain area can create substantial variations in the relationship between drainage area and floodplain width (e.g., Wohl et al., 2017). Greater drainage areas are more likely to have large flood magnitudes and therefore increasing disturbance of at least the channel-proximal portions of the floodplain, leading intuitively to the relationship with increased density. Wider floodplains are more likely to have portions farther from the contemporary active channel that have long turnover times (Konrad, 2012) and may experience homogenization through vegetation succession and prolonged vertical accretion, as reflected in greater aggregation for greater floodplain width ratios. These results suggest that geomorphically connected wider floodplains are very important to floodplain heterogeneity (Wohl, Lininger, et al., 2018).

The variables of average annual precipitation, mean floodplain elevation, and categorical flow regime were all chosen to constrain discharge characteristics. The results show that (a) aggregation increases with elevation, (b) aggregation is higher for rainfall-dominated flow, and (c) evenness increases with precipitation. We expect increasing elevation to correspond with greater likelihood of snowmelt-dominated flow and therefore less flashy systems and less floodplain disturbance due to colder winters. We see this reflected in aggregation increasing with elevation but not with higher aggregation for rainfall versus snowmelt. This suggests that elevation may not be an effective proxy for snowmelt versus rainfall dominated flow, and that the relationship between aggregation and elevation could more strongly reflect other vegetation dynamics rather than fluvial disturbances caused by different flow regimes. Lower aggregation for snowmelt systems could be due to the shorter growing season and reduced time for vegetation succession each year, resulting in less aggregated areas of vegetation. Evenness increasing with precipitation could reflect more evenly distributed resources for vegetation through higher groundwater levels across the floodplain (Zeng et al., 2019). Clearly, the relationships between elevation, precipitation, and flow regime need more study. Future study could use other proxies for flow regime, such as annual mean and range of temperature paired with precipitation and snow water equivalent, or direct measurements of flow regime such as mean annual flow, maximum annual flow, and base flow.

Large wood volume exerts an important influence on floodplain heterogeneity and is related to heterogeneity by (a) explaining 77% of the variability in interspersion and juxtaposition and (b) increasing density with LWV. It makes intuitive sense that large wood would increase density as wood can increase channel bifurcation and avulsion, island formation, planform complexity, and patchiness of floodplain forests (Collins et al., 2012). The primary effects of large wood in river corridors can be complex, however, as large wood can also reduce near-bank velocity and shear stress and reduce channel mobility (Daniels & Rhoads, 2003). Increasing the spatial detail of the large wood metric may shed light on the effects of large wood on floodplains, especially as large wood was once living trees and wood volumes reflect complex interactions between climate, habitat, and channel dynamics (Benda & Sias, 2003), shown simply in the strong positive relationship between precipitation and LWV (Table S3 in Supporting Information S1). This data set only includes wood volume per area from a limited number of transects and does not include the spatial distribution or concentration (e.g., jams) of the wood on the floodplain. Wood loads can be dynamic in space and time (Iroumé et al., 2015; Ruiz-Villanueva et al., 2016; Tonon et al., 2017; Wohl et al., 2019; Wohl, 2013) and the distribution of wood in a channel or floodplain can change substantially over 1–2 years (Wohl and Iskin, 2022). This highlights the need for more detailed study of large wood on floodplains to determine its effect on fluvial processes as related to floodplain heterogeneity. Isolating the category of large wood and including characteristics such as percentage of wood load in jams versus individual pieces, average distance between floodplain jams, average piece diameter, average piece length, and piece decay and/or burn class may allow for a more detailed understanding of the relationship between large wood and floodplain heterogeneity.

6. Conclusions

The results show that different facets of floodplain heterogeneity can be quantified with metrics from landscape ecology and that the patterns across the United States are varied and related to complex and dynamic fluvial processes. Although floodplain heterogeneity is a complex concept, there are some emergent trends from the

LOOCV model results that are easily interpretable, even with a sample size of 15. Qualitatively, we find that space available (measured by drainage area and floodplain/channel width ratio) and channel mobility (measured by channel planform and flow regime) are related to floodplain heterogeneity, and that natural floodplains in the United States have moderate aggregation, high interspersion and evenness, and a range of patch densities. Quantitatively, we find that drainage area, elevation, total sinuosity, floodplain width ratio, LWV, planform, and flow regime all influence floodplain heterogeneity and can explain 45%–77% of the variability in aggregation, interspersion, patch density, and evenness.

These findings can inform how river corridors can be managed to protect the processes that create and maintain floodplain heterogeneity, and how floodplains might change due to climate change. River corridor management and restoration can benefit from knowing the main controls of floodplain heterogeneity. Although management and restoration cannot target drainage area, elevation, or precipitation, they can target aspects related to natural flow, sediment, and wood regimes that affect sinuosity, floodplain width ratio, LWV, planform, and flow regime. Climate change is predicted to affect all the controls of floodplain heterogeneity, especially species distribution across latitude and elevation (Gray & Hamann, 2013) and habitat refugia (Michalak et al., 2018). The predicted effects of climate change are complex, and the results of this study highlight the need for additional investigation into how climate change will specifically affect floodplains and functional heterogeneity that sustain river ecosystems.

For natural corridors, we highlight the fact that it is difficult to isolate individual characteristics from each other (such as flow regime and elevation), because they commonly have dependent effects and are controlled by currently unidentified thresholds. The results presented here represent the beginning of cross-site investigations into floodplain heterogeneity. Future research could usefully focus on natural sites where it is possible to keep all/most of the characteristics consistent except for the variable of interest and compare floodplain heterogeneity related to that specific variable. For example, the Dinwoody Creek and Downs Fork sites in Wyoming occur adjacent to each other, so they have similar latitudes, elevations, precipitation, and flow regimes. The main distinguishing factor for these sites is that Dinwoody Creek has a straight planform, whereas Downs Fork has a history of glacier-outburst floods, creating an anastomosing planform. Searching for sites like these would be an effective way to investigate the effects of specific controls on floodplain spatial heterogeneity.

Future directions building from this research include increasing the breadth and depth of the data set. Increasing breadth includes (a) expanding the data set in the United States, such as including streams from the Southwest and Northeast, (b) expanding the data set globally to include natural rivers where sufficient elevation data are available, and (c) adding degraded sites to compare heterogeneity between impacted and natural floodplains. Adding sites that have been altered by human use might facilitate the delineation of metric thresholds for natural sites and provide more detail into natural versus altered levels of heterogeneity.

Our results only begin to identify the variables that influence floodplain heterogeneity, but no single measure of heterogeneity can capture the variability seen in the four metrics used in this study. We recommend that practitioners focus on measuring large wood characteristics and investigating historical planforms and sinuosity values as they relate to fluvial processes relevant to a specific site and consider measuring and monitoring interspersion and patch density, as they are the most readily understandable and interpretable metrics. Our hope is that this is just the beginning of a body of work that investigates the relationship between floodplain heterogeneity, connectivity, and fluvial processes, with the goal of protecting, improving, and restoring our river systems.

Data Availability Statement

The original field data collected for this study for West Bijou Creek, East Plum Creek, Rough and Tumbling Creek, Sand Creek, Hoh River, Sol Duc River, Lookout Creek, Altamaha River, North St. Vrain Creek, Congaree River, Embarras River, Swan River, Downs Fork, and Dinwoody Creek and floodplain delineation shapefiles for all sites are publicly available through Dryad (Iskin & Wohl, 2023a). For Yukon River delineation data, refer to Lininger et al. (2019), and for Yukon River wood data, refer to Lininger et al. (2017). Kimberly Meitzen provided the Congaree River National Park shapefile. Preliminary Swan River green lidar was used in this study (NCALM, 2023) and will be published by NCALM once finalized. The National Map (USGS, 2016, 2023c), the Washington Lidar Portal (Division of Geology and Earth Resources, 2022), the Colorado Hazard Mapping & Risk MAP Portal (CWCB, 2023), and OKMaps (Oklahoma Office of Geographic Information, 2023) were

used to download lidar files. StreamStats (USGS, 2023b) was used to delineate drainage areas, the National Water Dashboard (USGS, 2023a) was used to inspect annual streamflow patterns, Google Earth Engine (Gorelick et al., 2017) was used to create and download Sentinel-2A raster mosaics (links to the code provided in Supporting Information S1), ArcGIS Pro (Esri, 2022) was used to visualize and process the data and run the classification workflow, and R (R Core Team, 2023) was used to conduct the statistical analyses.

Acknowledgments
The authors thank Colorado Parks and Wildlife, the Geological Society of America, American Water Resources Association Colorado, and the Colorado Scientific Society for funding awarded to this project. We would also like to thank Samantha Pearson, Olivia Cecil, Meggie Olsen, Kristen Cognac, Logan Rutt, Daniel White, and Sarah Hinshaw for field work assistance. Thank you to Christi Lambert at The Nature Conservancy for assistance with background information for and access at the Altamaha River, Mark Schulze at HJ Andrews Experimental Forest for assistance with background information for Lookout Creek, Katherine Lininger at the University of Colorado Boulder for providing Yukon River floodplain delineations and large wood load data, The National Center for Airborne Laser Mapping (NCALM) for providing preliminary green lidar for the Swan River, Kimberly Meitzen at Texas State University for providing Congaree River DEM and park boundary data, and Max Ross at Olympic National Park for providing provisional soil data for the Hoh and Sol Duc Rivers. Thank you also to Kelly Bodwin at California Polytechnic State University, San Luis Obispo for R coding assistance and LOOCV method assistance, Brianna Rick at the Alaska Climate Adaptation Science Center for Google Earth Engine coding assistance, Ann Hess at Colorado State University for providing input on statistical interpretation, and Kyle Horton at Colorado State University for providing review and input on Figure S1 in Supporting Information S1. We acknowledge the National Park Service for access to Olympic National Park under permit OLYM-2021-SCI-0044. Facilities were provided by the HJ Andrews Experimental Forest and Long Term Ecological Research (LTER) program, administered cooperatively by Oregon State University, the USDA Forest Service Pacific Northwest Research Station, and the Willamette National Forest. Facilities were also provided by the Flathead Lake Biological Station operated by the University of Montana. I acknowledge The Nature Conservancy, Arapahoe County Open Spaces, and the Swan River State Forest for access to Sand Creek, West Bijou Creek, and the Swan River, respectively. This paper was improved by comments from two anonymous reviewers.

References

Aguiar, F. C., Ferreira, M. T. A., & Segurado, P. (2009). Structural and functional responses of riparian vegetation to human disturbance: Performance and spatial scale-dependence. *Fundamental and Applied Limnology*, *175*(3), 249–267. https://doi.org/10.1127/1863-9135/2009/0175-0249

Amoros, C., & Bornette, G. (2002). Connectivity and biocomplexity in waterbodies of riverine floodplains. *Freshwater Biology*, *47*(4), 761–776. https://doi.org/10.1046/j.1365-2427.2002.00905.x

Appling, A. P., Bernhardt, E. S., & Stanford, J. A. (2014). Floodplain biogeochemical mosaics: A multidimensional view of alluvial soils. *Journal of Geophysical Research: Biogeosciences*, *119*(8), 1538–1553. https://doi.org/10.1002/2013JG002543

Arscott, D. B., Tockner, K., van der Nat, D., & Ward, J. V. (2002). Aquatic habitat dynamics along a braided alpine river ecosystem (Tagliamento River, northeast Italy). *Ecosystems*, *5*, 802–814. https://doi.org/10.1007/s10021-002-0192-7

Ashmore, P. (2009). Intensity and characteristic length of braided channel patterns. *Canadian Journal of Civil Engineering*, *36*(10), 1656–1666. https://doi.org/10.1139/L09-088

Baartman, J. E. M., Masselink, R., Keesstra, S. D., & Temme, A. J. A. M. (2013). Linking landscape morphological complexity and sediment connectivity. *Earth Surface Processes and Landforms*, *38*(12), 1457–1471. https://doi.org/10.1002/esp.3434

Barry, R., Chorley, R., Barry, R. G., & Chorley, T. late R. (2004). *Atmosphere, weather and climate* (8th ed.). Routledge. https://doi.org/10.4324/9780203428238

Beighley, R. E., & Gummadi, V. (2011). Developing channel and floodplain dimensions with limited data: A case study in the Amazon Basin. *Earth Surface Processes and Landforms*, *36*(8), 1059–1071. https://doi.org/10.1002/esp.2132

Bellmore, J. R., & Baxter, C. V. (2014). Effects of geomorphic process domains on river ecosystems: A comparison of floodplain and confined valley segments. *River Research and Applications*, *30*(5), 617–630. https://doi.org/10.1002/rra.2672

Bellmore, J. R., Baxter, C. V., Martens, K., & Connolly, P. J. (2013). The floodplain food web mosaic: A study of its importance to salmon and steelhead with implications for their recovery. *Ecological Applications*, *23*(1), 189–207. https://doi.org/10.1890/12-0806.1

Benda, L. E., & Sias, J. C. (2003). A quantitative framework for evaluating the mass balance of in-stream organic debris. *Forest Ecology and Management*, *172*, 1–16. https://doi.org/10.1016/S0378-1127(01)00576-X

Benke, A. C. (2001). Importance of flood regime to invertebrate habitat in an unregulated river – Floodplain ecosystem. *Journal of the North American Benthological Society*, *20*(2), 225–240. https://doi.org/10.2307/1468318

Bhowmik, N. G. (1984). Hydraulic geometry of floodplains. *Journal of Hydrology*, *68*(1–4), 369–374. 377–401. https://doi.org/10.1016/0022-1694(84)90221-X

Bivand, R., Keitt, T., & Rowlingson, B. (2023). rgdal: Bindings for the "geospatial" data abstraction library. Version 1.6-4. Retrieved from https://cran.r-project.org/package=rgdal

Choné, G., & Biron, P. M. (2016). Assessing the relationship between river mobility and habitat. *River Research and Applications*, *32*(4), 528–539. https://doi.org/10.1002/rra.2896

Ciszewski, D., & Grygar, T. M. (2016). A review of flood-related storage and remobilization of heavy metal pollutants in river systems. *Water, Air, & Soil Pollution*, *227*(7), 239. https://doi.org/10.1007/s11270-016-2934-8

Collins, B. D., Montgomery, D. R., Fetherston, K. L., & Abbe, T. B. (2012). The floodplain large-wood cycle hypothesis: A mechanism for the physical and biotic structuring of temperate forested alluvial valleys in the North Pacific coastal ecoregion. *Geomorphology*, *139–140*, 460–470. https://doi.org/10.1016/j.geomorph.2011.11.011

Colorado Water Conservation Board (CWCB). (2023). Colorado hazard mapping & risk MAP portal [Software: Online program that visualizes and assists download of lidar data for the state of Colorado]. Retrieved from https://coloradohazardmapping.com/lidarDownload

Constantine, J. A., Dunne, T., Ahmed, J., Legleiter, C., & Lazarus, E. D. (2014). Sediment supply as a driver of river meandering and floodplain evolution in the Amazon Basin. *Nature Geoscience*, *7*(12), 899–903. https://doi.org/10.1038/ngeo2282

Daniels, M. D., & Rhoads, B. L. (2003). Influence of a large woody debris obstruction on three-dimensional flow structure in a meander bend. *Geomorphology*, *51*(1–3), 159–173. https://doi.org/10.1016/S0169-555X(02)00334-3

Dinno, A. (2017). dunn.test: Dunn's test of multiple comparisons using rank sums. Version 1.3.5. Retrieved from https://CRAN.R-project.org/package=dunn.test

Division of Geology and Earth Resources. (2022). Washington LiDAR portal [Software: Online program that visualizes and assists download of lidar data for the state of Washington]. Washington State Department of Natural Resources. Retrieved from https://lidarportal.dnr.wa.gov/

Doering, M., Freimann, R., Antenen, N., Roschi, A., Robinson, C. T., Rezzonico, F., et al. (2021). Microbial communities in floodplain ecosystems in relation to altered flow regimes and experimental flooding. *Science of the Total Environment*, *788*, 147497. https://doi.org/10.1016/j.scitotenv.2021.147497

Esri. (2022). ArcGIS Pro [Software: Graphical information systems]. Retrieved from https://www.esri.com/en-us/arcgis/products/arcgis-pro/overview

Esri. (2023). Watershed (ready to use). ArcGIS Pro 3.0 Help: Hydrology toolset. Retrieved from https://pro.arcgis.com/en/pro-app/latest/tool-reference/ready-to-use/watershed.htm

Everitt, B. L. (1968). Use of the cottonwood in an investigation of the recent history of a flood plain. *American Journal of Science*, *266*(6), 417–439. https://doi.org/10.2475/ajs.266.6.417

Fox, J., & Weisberg, S. (2019). *An {R} companion to applied regression* (3rd ed.). Sage. Retrieved from https://socialsciences.mcmaster.ca/jfox/Books/Companion/

Friedman, J. M., & Lee, V. J. (2002). Extreme floods, channel change, and riparian forests along ephemeral streams. *Ecological Monographs*, *72*(3), 409–425. https://doi.org/10.1890/0012-9615(2002)072[0409:EFCCAR]2.0.CO;2

Fuchs, J. W., Fox, G. A., Storm, D. E., Penn, C. J., & Brown, G. O. (2009). Subsurface transport of phosphorus in riparian floodplains: Influence of preferential flow paths. *Journal of Environmental Quality*, *38*(2), 473–484. https://doi.org/10.2134/jeq2008.0201

Gorelick, N., Hancher, M., Dixon, M., Ilyushchenko, S., Thau, D., & Moore, R. (2017). Google Earth Engine: Planetary-scale geospatial analysis for everyone. *Remote Sensing of the Environment*, *202*, 18–27. https://doi.org/10.1016/j.rse.2017.06.031

Graf, W. L. (2006). Downstream hydrologic and geomorphic effects of large dams on American rivers. *Geomorphology*, *79*(3–4), 336–360. https://doi.org/10.1016/j.geomorph.2006.06.022

Gray, L. K., & Hamann, A. (2013). Tracking suitable habitat for tree populations under climate change in western North America. *Climatic Change*, *117*(1–2), 289–303. https://doi.org/10.1007/s10584-012-0548-8

Güneralp, İ., & Rhoads, B. L. (2011). Influence of floodplain erosional heterogeneity on planform complexity of meandering rivers. *Geophysical Research Letters*, *38*(14), L14401. https://doi.org/10.1029/2011GL048134

He, H. S., Dezonia, B. E., & Mladenoff, D. J. (2000). An aggregation index (AI) to quantify spatial patterns of landscapes. *Landscape Ecology*, *15*(7), 591–601. https://doi.org/10.1023/A:1008102521322

Helton, A. M., Poole, G. C., Payn, R. A., Izurieta, C., & Stanford, J. A. (2014). Relative influences of the river channel, floodplain surface, and alluvial aquifer on simulated hydrologic residence time in a montane river floodplain. *Geomorphology*, *205*, 17–26. https://doi.org/10.1016/j.geomorph.2012.01.004

Hesselbarth, M. H. K., Sciaini, M., Nowosad, J., Hanss, S., Graham, L. J., Hollister, J., & With, K. A. (2022). Package "landscapemetrics" reference manual. Retrieved from https://cran.r-project.org/web/packages/landscapemetrics/

Hesselbarth, M. H. K., Sciaini, M., With, K. A., Wiegand, K., & Nowosad, J. (2019). landscapemetrics: An open-source R tool to calculate landscape metrics. *Ecography*, *42*(10), 1648–1657. https://doi.org/10.1111/ecog.04617

Hijmans, R. J. (2023). raster: Geographic data analysis and modeling. Version 3.6–14. Retrieved from https://cran.r-project.org/package=raster

Hong, L. B., & Davies, T. R. H. (1979). A study of stream braiding. *Geological Society of America Bulletin Part II*, *90*(12_Part_II), 1839–1859. https://doi.org/10.1130/gsab-p2-90-1839

Hopkins, K. G., Noe, G. B., Franco, F., Pindilli, E. J., Gordon, S., Metes, M. J., et al. (2018). A method to quantify and value floodplain sediment and nutrient retention ecosystem services. *Journal of Environmental Management*, *220*, 65–76. https://doi.org/10.1016/j.jenvman.2018.05.013

Hothorn, T., Hornik, K., van de Wiel, M. A., & Zeileis, A. (2008). Implementing a class of permutation tests: The coin package. *Journal of Statistical Software*, *28*(8), 1–23. https://doi.org/10.18637/jss.v028.i08

Huang, C., Geiger, E. L., & Kupfer, J. A. (2006). Sensitivity of landscape metrics to classification scheme. *International Journal of Remote Sensing*, *27*(14), 2927–2948. https://doi.org/10.1080/01431160600554330

Hughes, F. M. R. (1997). Floodplain biogeomorphology. *Progress in Physical Geography: Earth and Environment*, *21*(4), 501–529. https://doi.org/10.1177/030913339702100402

Iroumé, A., Mao, L., Andreoli, A., Ulloa, H., & Ardiles, M. P. (2015). Large wood mobility processes in low-order Chilean river channels. *Geomorphology*, *228*, 681–693. https://doi.org/10.1016/j.geomorph.2014.10.025

Iskin, E. P. (2023). Beyond the case study: Characterizing natural floodplain heterogeneity in the United States (PhD dissertation). Colorado State University. ProQuest Dissertations Publishing, 30315421. Retrieved from https://www.proquest.com/dissertations-theses/beyond-case-study-characterizing-natural/docview/2820206748/se-2?accountid=9649

Iskin, E. P., & Wohl, E. (2021). Wildfire and the patterns of floodplain large wood on the Merced River, Yosemite National Park, California, USA. *Geomorphology*, *389*, 107805. https://doi.org/10.1016/j.geomorph.2021.107805

Iskin, E. P., & Wohl, E. (2023a). Data associated with "Beyond the Case Study: Characterizing natural floodplain heterogeneity in the United States" [Dataset]. Dryad. https://doi.org/10.5061/dryad.0k6djhb4q

Iskin, E. P., & Wohl, E. (2023b). Quantifying floodplain heterogeneity with field observation, remote sensing, and landscape ecology: Methods and metrics. *River Research and Applications*, *39*(5), 911–929. https://doi.org/10.1002/rra.4109

Jeffres, C. A., Opperman, J. J., & Moyle, P. B. (2008). Ephemeral floodplain habitats provide best growth conditions for juvenile Chinook salmon in a California river. *Environmental Biology of Fishes*, *83*(4), 449–458. https://doi.org/10.1007/s10641-008-9367-1

Jeffries, R., Darby, S. E., & Sear, D. A. (2003). The influence of vegetation and organic debris on flood-plain sediment dynamics: Case study of a low-order stream in the New Forest, England. *Geomorphology*, *51*(1–3), 61–80. https://doi.org/10.1016/S0169-555X(02)00325-2

Junk, W. J., Bayley, P. B., & Sparks, R. E. (1989). The flood pulse concept in river-floodplain systems. In D. P. Dodge (Ed.), *Proceedings of the International Large River Symposium (LARS)* (pp. 110–127). Canadian Special Publication of Fisheries and Aquatic Sciences Special Publication 106.

Junk, W. J., & Piedade, M. T. F. (2010). An introduction to South American wetland forests: Distribution, definitions and general characterization. In W. Junk, M. Piedade, F. Wittmann, J. Schöngart, & P. Parolin (Eds.), *Amazonian floodplain forests. Ecological studies* (Vol. 210). Springer. https://doi.org/10.1007/978-90-481-8725-6_1

Kleindl, W. J., Rains, M. C., Marshall, L. A., & Hauer, F. R. (2015). Fire and flood expand the floodplain shifting habitat mosaic concept. *Freshwater Science*, *34*(4), 1366–1382. https://doi.org/10.1086/684016

Konrad, C. P. (2012). Reoccupation of floodplains by rivers and its relation to the age structure of floodplain vegetation. *Journal of Geophysical Research*, *117*(G4), G00N13. https://doi.org/10.1029/2011JG001906

Kuhn, M., & Wickham, H. (2020). Tidymodels: A collection of packages for modeling and machine learning using tidyverse principles. Retrieved from https://www.tidymodels.org

Lamigueiro, O. P., & Hijmans, R. (2023). rasterVis. Version 0.51.5. Retrieved from https://oscarperpinan.github.io/rastervis/

Larsen, A., Larsen, J. R., & Lane, S. N. (2021). Dam builders and their works: Beaver influences on the structure and function of river corridor hydrology, geomorphology, biogeochemistry and ecosystems. *Earth-Science Reviews*, *218*, 103623. https://doi.org/10.1016/j.earscirev.2021.103623

Larsen, L. G., & Harvey, J. W. (2010). How vegetation and sediment transport feedbacks drive landscape change in the Everglades and wetlands worldwide. *American Naturalist*, *176*(3), E66–E79. https://doi.org/10.1086/655215

Laurel, D., & Wohl, E. (2019). The persistence of beaver-induced geomorphic heterogeneity and organic carbon stock in river corridors. *Earth Surface Processes and Landforms*, *44*(1), 342–353. https://doi.org/10.1002/esp.4486

Lininger, K. B., Wohl, E., & Rose, J. R. (2018). Geomorphic controls on floodplain soil organic carbon in the Yukon Flats, Interior Alaska, from reach to river basin scales. *Water Resources Research*, *54*(3), 1934–1951. https://doi.org/10.1002/2017WR022042

Lininger, K. B., Wohl, E., Rose, J. R., & Leisz, S. J. (2019). Significant floodplain soil organic carbon storage along a large high-latitude river and its tributaries. *Geophysical Research Letters*, *46*(4), 2121–2129. https://doi.org/10.1029/2018GL080996

Lininger, K. B., Wohl, E., Sutfin, N. A., & Rose, J. R. (2017). Floodplain downed wood volumes: A comparison across three biomes. *Earth Surface Processes and Landforms*, *42*(8), 1248–1261. https://doi.org/10.1002/esp.4072

Lowell, J. L., Gordon, N., Engstrom, D., Stanford, J. A., Holben, W. E., & Gannon, J. E. (2009). Habitat heterogeneity and associated microbial community structure in a small-scale floodplain hyporheic flow path. *Microbial Ecology*, *58*(3), 611–620. https://doi.org/10.1007/s00248-009-9525-9

McGarigal, K., & Marks, B. J. (1995). FRAGSTATS: Spatial pattern analysis program for quantifying landscape structure. U.S. Forest Service General Technical Report PNW-GTR-351. Portland. https://doi.org/10.2737/PNW-GTR-351

Mertes, L. A. K., Dunne, T., & Martinelli, L. A. (1996). Channel-Floodplain geomorphology along the Solimões-Amazon river, Brazil. *Geological Society of America Bulletin*, *108*(9), 1089–1107. https://doi.org/10.1130/0016-7606(1996)108<1089:CFGATS>2.3.CO;2

Miall, A. D. (1997). A review of the braided-river depositional environment. *Earth-Science Reviews*, *13*(1), 1–62. https://doi.org/10.1016/0012-8252(77)90055-1

Michalak, J. L., Lawler, J. J., Roberts, D. R., & Carroll, C. (2018). Distribution and protection of climate refugia in North America. *Conservation Biology*, *32*(6), 1414–1428. https://doi.org/10.1111/cobi.13130

Naiman, R. J., Bechtold, J. S., Drake, D. C., Latterell, J. J., O'Keefe, T. C., & Balian, E. V. (2005). Origins, patterns, and importance of heterogeneity in riparian systems. In G. M. Lovett, M. G. Turner, C. G. Jones, & K. C. Weathers (Eds.), *Ecosystem function in heterogeneous landscapes* (pp. 279–309). Springer Science + Business Media, Inc. https://doi.org/10.1007/0-387-24091-8_14

National Center for Airborne Laser Mapping (NCALM). (2023). Preliminary Swan River green LiDAR DEM without bathymetric correction (1 m) [Dataset]. Retrieved from http://calm.geo.berkeley.edu/ncalm/dtc.html

Oklahoma Office of Geographic Information. (2023). OKMaps [Software: Online program that visualizes and assists download of lidar and other data for the state of Oklahoma]. Retrieved from https://okmaps.org/ogi/search.aspx

Omernik, J. M. (1987). Ecoregions of the conterminous United States. Map (scale 1:7,500,000). *Annals of the Association of American Geographers*, *77*(1), 118–125. https://doi.org/10.1111/j.1467-8306.1987.tb00149.x

Petsch, D. K., Cioneck, V. D., Thomaz, S. M., & dos Santos, N. C. L. (2022). Ecosystem services provided by river-floodplain ecosystem. *Hydrobiologia*, *850*(12–13), 2563–2584. https://doi.org/10.1007/s10750-022-04916-7

PRISM Climate Group (PRISM). (2002). Western Canada average annual precipitation, 1961-1990 (2km; ASCIWe Grid) [Dataset: Averaged precipitation data for Western Canada]. Oregon State University. Retrieved from https://prism.oregonstate.edu/projects/canw.php

PRISM Climate Group (PRISM). (2018). Alaska average annual precipitation, 1981-2010 (800m; ASCIWe Grid) [Dataset: Precipitation data for the state of Alaska]. Oregon State University. Retrieved from https://prism.oregonstate.edu/projects/alaska.php

PRISM Climate Group (PRISM). (2022). United States average total precipitation, 1991-2020 (800m; ASCIWe Grid) [Dataset: Precipitation data for the continental United States]. Oregon State University. Retrieved from https://prism.oregonstate.edu/normals/

R Core Team. (2023). R: A language and environment for statistical computing [Software: Open source software used for data visualization and statistical analyses]. Retrieved from https://www.r-project.org/

Ruiz-Villanueva, V., Piégay, H., Gaertner, V., Perret, F., & Stoffel, M. (2016). Wood density and moisture sorption and its influence on large wood mobility in rivers. *CATENA*, *140*, 182–194. https://doi.org/10.1016/j.catena.2016.02.001

Samaritani, E., Shrestha, J., Fournier, B., Frossard, E., Gillet, F., Guenat, C., et al. (2011). Heterogeneity of soil carbon pools and fluxes in a channelized and a restored floodplain section (Thur River, Switzerland). *Hydrology and Earth System Sciences*, *15*(6), 1757–1769. https://doi.org/10.5194/hess-15-1757-2011

Schumm, S. A. (1985). Patterns of Alluvial Rivers. *Annual Review of Earth and Planetary Sciences*, *13*(1), 5–27. https://doi.org/10.1146/annurev.ea.13.050185.000253

Schwendel, A. C., Nicholas, A. P., Aalto, R. E., Sambrook Smith, G. H., & Buckley, S. (2015). Interaction between meander dynamics and floodplain heterogeneity in a large tropical sand-bed river: The Rio Beni, Bolivian Amazon. *Earth Surface Processes and Landforms*, *40*(15), 2026–2040. https://doi.org/10.1002/esp.3777

Scott, D. T., Gomez-Velez, J. D., Jones, C. N., & Harvey, J. W. (2019). Floodplain inundation spectrum across the United States. *Nature Communications*, *10*(1), 5194. https://doi.org/10.1038/s41467-019-13184-4

Scott, M. L., Friedman, J. M., & Auble, G. T. (1996). Fluvial process and the establishment of bottomland trees. *Geomorphology*, *14*(4), 327–339. https://doi.org/10.1016/0169-555X(95)00046-8

Scown, M. W., Thoms, M. C., & de Jager, N. R. (2015). Measuring floodplain spatial patterns using continuous surface metrics at multiple scales. *Geomorphology*, *245*, 87–101. https://doi.org/10.1016/j.geomorph.2015.05.026

Scown, M. W., Thoms, M. C., & de Jager, N. R. (2016a). An index of floodplain surface complexity. *Hydrology and Earth System Sciences*, *20*(1), 431–441. https://doi.org/10.5194/hess-20-431-2016

Scown, M. W., Thoms, M. C., & de Jager, N. R. (2016b). Measuring spatial patterns in floodplains: A step towards understanding the complexity of floodplain ecosystems. In D. J. Gilvear, M. T. Greenwood, M. C. Thoms, & P. J. Wood (Eds.), *River science: Research and management for the 21st century* (pp. 103–131). John Wiley & Sons, Ltd. https://doi.org/10.1002/9781118643525.ch6

Skalak, K., & Pizzuto, J. (2010). The distribution and residence time of suspended sediment stored within the channel margins of a gravel-bed bedrock river. *Earth Surface Processes and Landforms*, *35*(4), 435–446. https://doi.org/10.1002/esp.1926

Stanford, J. A., Lorang, M. S., & Hauer, F. R. (2005). The shifting habitat mosaic of river ecosystems. *SIL Proceedings, 1922–2010*, *29*(1), 123–136. https://doi.org/10.1080/03680770.2005.11901979

Stella, J. C., Hayden, M. K., Battles, J. J., Piégay, H., Dufour, S., & Fremier, A. K. (2011). The role of abandoned channels as refugia for sustaining pioneer riparian forest ecosystems. *Ecosystems*, *14*(5), 776–790. https://doi.org/10.1007/s10021-011-9446-6

Stoffers, T., Buijse, A. D., Verreth, J. A. J., & Nagelkerke, L. A. J. (2022). Environmental requirements and heterogeneity of rheophilic fish nursery habitats in European lowland rivers: Current insights and future challenges. *Fish and Fisheries*, *23*(1), 162–182. https://doi.org/10.1111/faf.12606

Sutfin, N. A., & Wohl, E. (2019). Elevational differences in hydrogeomorphic disturbance regime influence sediment residence times within mountain river corridors. *Nature Communications*, *10*(1), 2221. https://doi.org/10.1038/s41467-019-09864-w

Tockner, K., Bunn, S. E., Gordon, C., Naiman, R. J., Quinn, G. P., & Stanford, J. A. (2008). Flood plains: Critically threatened ecosystems. In N. Polunin (Ed.), *Aquatic ecosystems: Trends and global prospects* (pp. 45–62). Cambridge University Press. https://doi.org/10.1017/CBO9780511751790.006

Tockner, K., Malard, F., & Ward, J. V. (2000). An extension of the flood pulse concept. *Hydrological Processes Special Issue: Linking Hydrology and Ecology*, *14*(16–17), 2861–2883. https://doi.org/10.1002/1099-1085(200011/12)14:16/17<2861::AID-HYP124>3.0.CO;2-F

Tonon, A., Iroumé, A., Picco, L., Oss-Cazzador, D., & Lenzi, M. A. (2017). Temporal variations of large wood abundance and mobility in the Blanco River affected by the Chaitén volcanic eruption, southern Chile. *CATENA*, *156*, 149–160. https://doi.org/10.1016/j.catena.2017.03.025

Uno, H. (2016). Stream thermal heterogeneity prolongs aquatic-terrestrial subsidy and enhances riparian spider growth. *Ecology*, *97*(10), 2547–2553. https://doi.org/10.1002/ecy.1552

Uno, H., Yokoi, M., Fukushima, K., Kanno, Y., Kishida, O., Mamiya, W., et al. (2022). Spatially variable hydrological and biological processes shape diverse post-flood aquatic communities. *Freshwater Biology*, *67*(3), 549–563. https://doi.org/10.1111/fwb.13862

U.S. Geological Survey (USGS). (2016). McKenzie river bare earth mosaic [Dataset: Bare earth mosaic of the McKenzie River near Blue River, Oregon]. Retrieved from http://prd-tnm.s3.amazonaws.com/index.html?prefix=StagedProducts/Elevation/metadata/OR_McKenzieRiver_2021_B21/OR_McKenzieRiver_1_2021/spatial_metadata/contractor_provided/

U.S. Geological Survey (USGS). (2023a). National water dashboard [Software: Online program that provides stream gage data]. Retrieved from https://dashboard.waterdata.usgs.gov/app/nwd
U.S. Geological Survey (USGS). (2023b). StreamStats [Software: Online program that delineates watersheds and provides basin-scale estimates]. Retrieved from https://streamstats.usgs.gov/ss/
U.S. Geological Survey (USGS). (2023c). The national map download client [Software: Online program that visualizes and assists download of lidar and other data]. Retrieved from https://apps.nationalmap.gov/downloader/
Van Wagner, C. E. (1968). The line intersect method in forests fuel sampling. *Forest Science*, *14*(1), 20–26.
Ward, J. V., Malard, F., & Tockner, K. (2002). Landscape ecology: A framework for integrating pattern and process in river corridors. *Landscape Ecology*, *17*(Suppl 1), 35–45. https://doi.org/10.1023/A:1015277626224
Westbrook, C. J., Cooper, D. J., & Baker, B. W. (2011). Beaver assisted river valley formation. *River Research and Applications*, *27*(2), 247–256. https://doi.org/10.1002/rra.1359
Wickham, H., Averick, M., Bryan, J., Chang, W., McGowan, L. D., François, R., et al. (2019). Welcome to the tidyverse. *Journal of Open Source Software*, *4*(43), 1686. https://doi.org/10.21105/joss.01686
Wohl, E. (2013). Floodplains and wood. *Earth-Science Reviews*, *123*, 194–212. https://doi.org/10.1016/j.earscirev.2013.04.009
Wohl, E. (2015). Particle dynamics: The continuum of bedrock to alluvial river segments. *Geomorphology*, *241*, 192–208. https://doi.org/10.1016/j.geomorph.2015.04.014
Wohl, E. (2021). An integrative conceptualization of floodplain storage. *Reviews of Geophysics*, *59*(2), e2020RG000724. https://doi.org/10.1029/2020rg000724
Wohl, E., & Cadol, D. (2011). Neighborhood matters: Patterns and controls on wood distribution in old-growth forest streams of the Colorado Front Range, USA. *Geomorphology*, *125*(1), 132–146. https://doi.org/10.1016/j.geomorph.2010.09.008
Wohl, E., & Iskin, E. P. (2019). Patterns of floodplain spatial heterogeneity in the southern Rockies, USA. *Geophysical Research Letters*, *46*(11), 5864–5870. https://doi.org/10.1029/2019GL083140
Wohl, E., & Iskin, E. P. (2022). The transience of channel-spanning logjams in mountain streams. *Water Resources Research*, *58*(5), e2021WR031556. https://doi.org/10.1029/2021WR031556
Wohl, E., Kramer, N., Ruiz-Villanueva, V., Scott, D. N., Comiti, F., Gurnell, A. M., et al. (2019). The natural wood regime in rivers. *BioScience*, *69*(4), 259–273. https://doi.org/10.1093/biosci/biz013
Wohl, E., Lininger, K. B., & Scott, D. N. (2018). River beads as a conceptual framework for building carbon storage and resilience to extreme climate events into river management. *Biogeochemistry*, *141*(3), 365–383. https://doi.org/10.1007/s10533-017-0397-7
Wohl, E., Polvi, L. E., & Cadol, D. (2011). Wood distribution along streams draining old-growth floodplain forests in Congaree National Park, South Carolina, USA. *Geomorphology*, *126*(1–2), 108–120. https://doi.org/10.1016/j.geomorph.2010.10.035
Wohl, E., Rathburn, S., Chignell, S., Garrett, K., Laurel, D., Livers, B., et al. (2017). Mapping longitudinal stream connectivity in the North St. Vrain Creek watershed of Colorado. *Geomorphology*, *277*, 171–181. https://doi.org/10.1016/j.geomorph.2016.05.004
Wohl, E., Scott, D. N., & Lininger, K. B. (2018). Spatial distribution of channel and floodplain large wood in forested river corridors of the Northern Rockies. *Water Resources Research*, *54*(10), 7879–7892. https://doi.org/10.1029/2018WR022750
Zeng, Y., Zhao, C., Li, J., Li, Y., Lu, G., & Liu, T. (2019). Effect of groundwater depth on riparian plant diversity along riverside-desert gradients in the Tarim River. *Journal of Plant Ecology*, *12*(3), 564–573. https://doi.org/10.1093/jpe/rty048
Zeug, S. C., & Winemiller, K. O. (2008). Relationships between hydrology, spatial heterogeneity, and fish recruitment dynamics in a temperate floodplain river. *River Research and Applications*, *24*(1), 90–102. https://doi.org/10.1002/rra.1061

References From the Supporting Information

Allison, S., & Martinez, D. (2013). Hoh River LiDAR-delivery 2 technical data report. Retrieved from https://pugetsoundlidar.ess.washington.edu/lidardata/proj_reports/Hoh_River_LiDAR_131104_Final_Report.pdf
European Space Agency (ESA). (2021). Level-2A. Sentinel online. Retrieved from https://sentinel.esa.int/web/sentinel/user-guides/sentinel-2-msi/product-types/level-2a
European Space Agency (ESA). (2023). Processing baseline. Sentinel online. Retrieved from https://sentinels.copernicus.eu/web/sentinel/technical-guides/sentinel-2-msi/processing-baseline
Gleason, A., & McWethy, G. (2014). Lidar project quality assurance report. Retrieved from https://lidarportal.dnr.wa.gov/#47.79332:-123.65662:10
Google Developers. (2022). Sentinel-2 MSI: MultiSpectral instrument, level-2A [Dataset: Bottom of atmosphere ESA Sentinel dataset]. Earth Engine Data Catalog. Retrieved from https://developers.google.com/earth-engine/datasets/catalog/COPERNICUS_S2_SR#bands
Open Topography. (2021). USGS 1/3 arc-second digital elevation model. https://doi.org/10.5069/G98K778D
Sabins, F. F., Jr., & Ellis, J. M. (2020). *Remote sensing: Principles, interpretation, and applications* (4th ed.). Waveland Press, Inc. Retrieved from https://www.waveland.com/browse.php?t=421